Published in final edited form as:
J Am Chem Soc. 2011 July 20; 133(28): 10752–10755. doi:10.1021/ja204155r.

Post-Self-Assembly Covalent Chemistry of Discrete Multicomponent Metallosupramolecular Hexagonal Prisms

Ming Wang, **Wen-Jie Lan**, **Yao-Rong Zheng**, **Timothy R. Cook**, **Henry S. White**, and **Peter J. Stang**
Department of Chemistry, University of Utah, 315 South 1400 East, Salt Lake City, Utah 84112

Peter J. Stang: stang@chem.utah.edu

Abstract

The multicomponent coordination-driven self-assembly of hexakis[4-(4-pyridyl)phenyl]benzene, *cis*-$(PEt_3)_2Pt^{II}(OTf)_2$, and amine- or maleimide-functionalized isophthalate forms discrete hexagonal prisms as single reaction products. The amino or maleimide groups decorating the isophthalate pillars of the prisms provide reactive sites for post self-assembly modifications. In this communication, we demonstrate that the hexagonal prisms can be functionalized without disrupting the prismatic cores, enabling the incorporation of new functionalities under mild conditions.

To effect and maintain biological functions, natural systems assemble a variety of specialized supramolecular nanostructures from multiple subunits with high efficiency. In the past two decades, coordination-driven self-assembly has emerged as an effective tool for constructing functionalized metallosupramolecules with the aim of better understanding and mimicking their biological analogs.[1] It has been well demonstrated that 2-D macrocycles and 3-D cages can form by the self-assembly of molecular subunits encoded with specific directional information[1] (controlling their sizes and shapes) and appropriate chemical functionalities[2] (tuning their physical and chemical properties). Such functionalized metallosupramolecules lend themselves to various applications, from supramolecular catalysis to chemical sensing and host-guest chemistry.[2, 3] Although the self-assembly of 2-D and 3-D supramolecules is possible by using pre-functionalized subunits, this strategy is hindered by the potential incompatibilities of the functionalities with the self-assembly process, thus limiting the library of possible building blocks. For example, for pyridyl-based cage formations, the use of carboxylate-functionalized ligands is problematic in that the carboxylate groups will compete with the pyridines for coordination to the metal nodes, thereby disrupting self-assembly.

Post-self-assembly modifications of supramolecules via covalent and non-covalent chemistry can be used to circumvent the problems associated with certain functional groups, unlocking the full potential of these structures. Nature routinely utilizes a post-self-assembly modification strategy in order to tune the structures and functionalities of biological scaffolds. For example, the post-translational modification of cellular proteins, accomplished through enzyme-catalyzed reactions, has expanded protein diversities and enables certain biological functions.[4] Recently, artificial post-assembly modification strategies have emerged which parallel nature's approach for forming functional

Correspondence to: Henry S. White; Peter J. Stang, stang@chem.utah.edu.

Supporting Information Available: Syntheses and analytical data for **5–10**; Cyclic voltammograms, steady-state measurements, chronoamperometry, calculations of D and θ_{sites}, and molecular modeling procedures. This material is available free of charge via the internet at http://pubs.acs.org.

supramolecules with specific properties. Metal-organic frameworks (MOFs) represent the most studied class of supramolecules which possess extraordinary properties as a result of post-synthetic modification reactions.[5–10] A variety of chemical methods have been employed to modify the organic components of MOFs and to engineer their surfaces, thus endowing or extending their applications in gas storage[7] and separation,[8] catalysis,[9] and drug delivery.[10] Despite the success of post-synthetic modifications in tuning the structures and functionalities of infinite MOFs, suitable and diverse post-synthetic modifications of discrete supramolecular structures to construct novel functionalized self-assemblies with unique properties have received less attention. In a rare example, Zhou et al. recently engineered the hydrophobic surface of a discrete metal-organic polyhedron to become hydrophilic through post-synthetic modifications, leading to the development of water-soluble nanocages to serve as drug carriers .[11]

Herein, we report the design and preparation of metallosupramolecular hexagonal prisms decorated with amine or maleimide groups via multicomponent coordination-driven self-assembly, wherein the free decorated groups of the prisms allow for efficient post-synthetic covalent modifications to incorporate new functionalities under mild conditions. First, we explored the selective formation of amine- or maleimide-decorated hexagonal prisms using heteroligation-directed multicomponent coordination-driven self-assembly.[12,13] As shown in Scheme 1 (*A*), the combination of hexakis[4-(4-pyridyl)phenyl]benzene (**1**), *cis*-$(PEt_3)_2Pt(OTf)_2$ (**2**), and 5-aminoisophthalate (**3**) or 5-maleimideisophthalate (**4**) induces the formation of discrete hexagonal prisms (**5** or **6**) as the sole products based on recently developed methodologies.[12,13] The amino groups of **3** are accessible upon formation of **5**, permitting facile reactions with isocyanate or maleic anhydride (Scheme 1, *B*) to illustrate covalent post-assembly modifications of the prism. Similarly, the maleimide groups tethered to the pillars of **6** can undergo Diels-Alder reactions with (9-methylene anthracenyl)-1-ferrocenoate (Scheme 1, *B*) as a post-assembly modification. Hexagonal prisms **7–10** were obtained in high yields after quantitative post-synthetic modifications of **5** or **6**, leading to the incorporation of new functionalities such as urea groups, alkenes, and carboxylic acids. In addition, the post-synthetic modification of **6** with ferrocene derivatives conferred redox features to **10**. All hexagonal prisms were characterized and supported by multinuclear NMR and electron-spray ionization mass spectrometry. Their sizes and shapes were established with molecular-force field simulations and further supported by PGSE NMR experiments.

Hexagonal prisms **5** and **6** self-assembled upon mixing **1**, **2,** and **3** or **4** in a 2:12:6 ratio in acetone/water (v:v = 8:1) followed by 2 h of stirring at 70 °C. The solvent was then removed *in vacuo* and the resulting residue redissolved in neat nitromethane-*d*3, followed by an additional 4 h of stirring at 70 °C. Solids **5** and **6** could be isolated in >90% yields from the resulting colorless solutions by removing all solvent under vacuum. The $^{31}P\{^1H\}$ and ^1H NMR multinuclear spectra of **5** and **6** indicated the formation of single, discrete structures with high symmetry. The $^{31}P\{^1H\}$ NMR spectrum of **5** and **6** displayed two doublets with approximately equal intensities at δ = 6.73 and 0.88 ppm ($^2J_{P\text{-}P}$ = 21.5 Hz) for **5**, 6.57 and 1.07 ppm ($^2J_{P\text{-}P}$ = 21.5 Hz) for **6**, corresponding to the two distinct phosphorous environments present (Figure 1 and S1, SI). These spectra are similar to those in our recent reports on the multicomponent self-assembly of tetragonal and hexagonal prisms.[12, 13] In the ^1H NMR spectra of **5** and **6** (Figure 1 and S1, SI), sharp signals corresponding to coordinated pyridine protons were identified around 8.60 and 7.60 ppm with small downfield shifts relative to **1**. The protons assigned to the isophthalate ligands were observed at δ = 7.19 and 7.11 for **5**, 7.84 and 7.90 ppm for **6.** In addition, signals at δ = 4.25 ppm (for **5**) and 6.92 ppm (for **6**) were identified to the protons of the amine and maleimide, respectively. The well-defined, sharp signals in both the $^{31}P\{^1H\}$ and ^1H NMR spectra support the exclusive formation of single products, consistent with hexagonal prismatic

structures. ESI-MS provides further evidence for the hexagonal prismatic nature of **5** and **6**. As shown in Figure 2 (*A*), peaks at 2358.4, 1856.7, 1522.6, 1157.8, 1104.7, and 854.2 corresponding to the fragments of $[M - 4OTf]^{4+}$, $[M - 5OTf]^{5+}$, $[M - 6OTf]^{6+}$, $[M - 7OTf]^{7+}$, $[M - 8OTf]^{8+}$, and $[M - 10OTf]^{10+}$ for **5** were observed. Furthermore, the peaks assigned to $[M - 5OTf]^{5+}$ of **5** and **6** were isotopically resolved and agreed well with their calculated theoretical distributions (Figure 2 and S2, SI).

Covalent post-synthetic modifications of **5** and **6** were achieved by treating **5** with isocyanate or maleic anhydride in a 1:10 ratio, **6** with (9-methylene anthracenyl)-1-ferrocenoate in a ratio of 1:5, respectively, in nitromethane*d*3 solutions, followed by 12 h of stirring at 90 °C. All solvent was then removed *in vacuo*. The resulting residues were redissolved in neat acetone and diethyl ether was added to afford hexagonal prisms **7–10** in yields exceeding 70%. The $^{31}P\{^{1}H\}$ and ^{1}H NMR spectra of **7–10** supported that the hexagonal prismatic core of **5** or **6** remained intact. For example, the $^{31}P\{^{1}H\}$ NMR spectrum of **7** displays two doublets at δ = 6.74, 0.95 ppm ($^{2}J_{P\text{-}P}$ = 21.2 Hz), similar to those of **5** (Figure 1, *A*), which correspond to the two unique phosphorous environments of the prism. The doublet at 0.95 ppm, assigned to the phosphorus atoms *trans* to the carboxylate ligand, displays a slight shift (Δδ = 0.07 ppm) compared to that of **5**. The $^{31}P\{^{1}H\}$ NMR spectra of **8–10** also display the two tell-tale doublets, diagnostic of the hexagonal prismatic core(Figure S3–S5, SI). The doublet in **9** which corresponds to the phosphine *trans* to the carboxylate shifts by 0.21 ppm. In the ^{1}H NMR spectrum of **7** (Figure 1, *B*), the signal ascribed to the amino group of **5** at δ = 4.25 was replaced with new peaks at δ = 5.56 and 8.49 ppm, indicating complete conversion of the amine into a urea functionality. In addition, the peaks assigned to the aromatic protons of isophthalate displayed obvious downfield shifts ($\Delta\delta_{H\text{-}a}$ = 0.29 ppm, $\Delta\delta_{H\text{-}b}$ = 0.80 ppm) compared to those of **5**. Furthermore, multiplets at δ = 3.78, 5.11, 5.22, and 5.90 ppm, arising from the allyl group, were observed. In the ^{1}H NMR spectra of **8–10** Figure S3–S5, SI), the signals corresponding to the protons of isophthalate displayed similar down-field shifts as in the case of **7**. Also, new peaks at δ = 5.39 and 8.49 ppm, ascribed to the urea group of **8**, and two doublets at δ = 6.40 and 6.63 ppm, ascribed to the olefin of **9**, δ = 5.61, 4.95, 4.85, 4.79, 4.53, and 4.37 ppm due to the cycloaddition of (9-methylene anthracenyl)-1-ferrocenoate for **10** were observed. Comparison of the $^{31}P\{^{1}H\}$ and ^{1}H NMR spectra of **5** or **6** with those of **7–10** indicate clearly that the amino or maleimide groups of hexagonal prism were modified in the presence of isocyanate, maleic anhydride, or anthracene derivatives, yielding new functionalized hexagonal prisms while maintaining the integrity of the prismatic core. ESI-MS data provide further evidence for the hexagonal prismatic structures of **7–10**. Figure 2(A) compares the full mass spectra of **5** and **7**. The peaks corresponding to **5** are absent in the mass spectrum of **7**, replaced by peaks corresponding to the fragments of $[M - 4OTf]^{4+}$, $[M - 5OTf]^{5+}$, $[M - 6OTf]^{6+}$, $[M - 8OTf]^{8+}$, and $[M - 11OTf]^{11+}$ for the new functionalized prism. Also, the peak assigned to $[M - 5OTf]^{5+}$ of **7** was isotopically resolved and in good agreement with its calculated theoretical distribution (Figure 2, B). Similar well-defined and isotopically-resolved peaks were observed in the mass spectra of **8–10** (Figure S6–S8, SI). These results firmly support the complete conversion of **5** or **6** into corresponding post-synthetically modified hexagonal prisms via covalent chemistry at the amino sites.

The post-synthetic modification of **6** with ferrocene derivatives confers electrochemical activity to the resulting functionalized hexagonal prism.[14] Cyclic voltammetry (CV) was performed on **6** and **10** using a ~0.5 mm^2 Pt disk electrode in acetonitrile with 0.1 M n-Bu_4NPF_6 as the supporting electrolyte. Figure 3A shows a single redox wave for **10**, suggesting no electronic intermolecular interaction among the multiple redox centers on the pillars.[15] No similar redox events were observed for **6** (Figure S9, SI), further verifying that the ferrocenyl groups were incorporated into **10**. Furthermore, the average potential difference between the anodic and cathodic peak potentials (ΔE_p) of **10** was 78.3 mV,

slightly larger than the theoretical value for an ideal reversible redox system (59 mV at 25 °C) due to the solution ohmic resistance. The anodic and cathodic peak currents observed for oxidation of **10** were equal, indicating chemical stability of oxidized **10** on the timescale of the voltammetric experiment.

The steady-state electrochemical properties of functionalized hexagonal prism **10** were also investigated on a ~25 μm diameter Pt disk electrode (Figure 3B). Voltammetric responses of **10** show hysteresis in the forward and reverse scans due to some absorption of oxidized **10** at the Pt electrode surface. The corresponding slopes of plots of E vs. $\log[(i_{lim}\text{-}i)/i]$ for **10** were approximately −64.5 mV/dec, where i_{lim} is the current limited by the mass transport of **10** (see Figure S10, SI). The similarity between the experimental and ideal value (−59 mV/n, n = 1) indicates the absence of strong intramolecular electronic-coupling between the ferrocene moieties.[16]

Finally, chronoamperometry measurements, as described by Denault and Bard,[17] were performed with the same Pt disk microelectrode to measure the diffusion coefficient (D) of the electroactive species **10**. The potential was stepped from a non-reaction potential (0.2 V vs. Ag/AgCl) to a diffusion-controlled potential (1.0 V) and the resulting time-dependent current (i_t) was continuously monitored. The slope at the long time region of the i_t/i_{lim} vs. $t_{-0.5}$ plot was used to estimate the D of **10** (see Figure S11, SI), 3.44×10^{-6} cm^2/s, close to that as determined by the pulsedgradient spin-echo (PGSE) method ($3.59 \times 10^{-6} \pm 8.0 \times 10^{-8}$ cm^2/s). This value was then used to determine the number of electroactive ferrocenyl groups on **10**, giving $\theta_{sites} \sim 6.5 \pm 0.5$, in good agreement with the expected value of 6 for a functionalized hexagonal prism in which all ferrocenes are active. We speculate that the small discrepancy may result from weak adsorption of **10**.

As attempts to grow single crystals of these hexagonal prisms suitable for X-ray crystallography have so far been unsuccessful, molecular force field simulations were used to gain further structural information about **5–10**. Molecular dynamic simulations using MMFF force fields were applied to independently equilibrate these self-assemblies, followed by energy minimizations of the resulting structures to full convergence. As shown in Figure 4 and S12 (SI), all of the computationally minimized structures are well-defined hexagonal prisms with approximate diameters around 2.60 nm, which are comparable to the sizes determined by PGSE experiments **5**: 2.66 ± 0.02 nm; **6**: 2.96 ± 0.03 nm; **7**:2.52 ± 0.02 nm; **8**: 2.84 ± 0.04 nm; **9**: 2.54 ± 0.02 nm; **10**: 3.18 ± 0.04 nm).

In summary, we report in this communication the facile and efficient covalent post-synthetic modification of hexagonal prisms decorated with amino or maleimide groups. The strategy developed here provides an alternative approach to access functionalized metallosupramolecules, especially useful for the formation of species which are not accessible via conventional coordination-driven self-assembly. This post-synthetic approach can impart new properties to the modified supramolecules as a way to unlock new applications and behaviors. For example, redox active functionalities can be incorporated onto the self-assemblies, as described here. We are currently extending this post-synthetic modification strategy towards the development of stimulus-responsive supramolecules.

Supplementary Material

Refer to Web version on PubMed Central for supplementary material.

Acknowledgments

P.J.S thanks the NIH (Grant GM-057052) for financial support. H.S.W thanks the NSF (Grant CHE CHE-0616505) for financial support.

References

1. (a) Stang PJ, Olenyuk B. Acc. Chem. Res. 1997; 30:502.(b) Leininger S, Olenyuk B, Stang PJ. Chem. Rev. 2000; 100:853. [PubMed: 11749254] (c) Seidel SR, Stang PJ. Acc. Chem. Res. 2002; 35:972. [PubMed: 12437322] (d) De S, Mahata K, Schmittel M. Chem. Soc. Rev. 2010; 39:1555. [PubMed: 20419210]
2. (a) Northrop BH, Yang H-B, Stang PJ. Chem. Commun. 2008:5896.(c) Parkash MJ, Lah MS. Chem. Commun. 2009:3326.(d) Pluth MD, Bergman RG, Raymond KN. Acc. Chem. Res. 2009; 42:1650. [PubMed: 19591461]
3. (a) Zheng YR, Zhao Z, Kim H, Wang M, Ghosh K, Pollock JB, Chi K-W, Stang PJ. Inorg. Chem. 2010; 49:12038.(b) Wang M, Vajpayee V, Shanmugaraju S, Zheng YR, Zhao Z, Hyunuk Kim, Mukherjee PS, Chi K-W, Stang PJ. Inorg. Chem. 2011; 50:1506. [PubMed: 21214171]
4. Richard C, Balavoine F, Schultz P, Ebbesen TW, Mioskowski C. Science. 2003; 300:775. [PubMed: 12730595]
5. (a) Wang ZQ, Cohen SM. Chem. Soc. Rev. 2009; 38:1315. [PubMed: 19384440] (b) Lee J, Farha OK, Roberts J, Scheidt KA, Nguyen ST, Hupp JT. Chem. Soc. Rev. 2009; 38:1450. [PubMed: 19384447] (c) Cohen SM. Chem. Sci. 2010; 1:32.(d) Tanabe KK, Cohen SM. Chem. Soc. Rev. 2011; 40:498. [PubMed: 21103601]
6. (a) Wang ZQ, Cohen SM. J. Am. Chem. Soc. 2007; 129:12368. [PubMed: 17880219] (b) Nguyen JG, Cohen SM. J. Am. Chem. Soc. 2010; 132:4560. [PubMed: 20232871] (c) Gadzikwa T, Lu G, Stern CL, Wilson SR, Hupp JT, Nguyen ST. Chem Commun. 2008:5493.
7. (a) Gadzikwa T, Farha OK, Malliakas CD, Kanatzidis MG, Hupp JT, Nguyen ST. J. Am. Chem. Soc. 2009; 131:13613. [PubMed: 19736982] (b) Tanabe KK, Wang ZQ, Cohen SM. J. Am. Chem. Soc. 2008; 130:8508. [PubMed: 18540671] (c) Doonan CJ, Morris W, Furukawa H, Yaghi OM. J. Am. Chem. Soc. 2009; 131:9492. [PubMed: 19534523] (d) Savonnet M, Bazer-Bachi D, Bats N, Perez-Pellitero J, Jeanneau E, Lecocq V, Pinel C, Farrusseng D. J. Am. Chem. Soc. 2010; 132:4518. [PubMed: 20232865]
8. (a) Gadzikwa T, Farha OK, Mulfort KL, Hupp JT, Nguyen ST. Chem. Commun. 2009:3720.(b) Burrows AD, Frost CG, Mahon MF, Richardson C. Angew. Chem. Int. Ed. 2008; 47:8482.
9. (a) Wu CD, Hu A, Zhang L, Lin W. J. Am. Chem. Soc. 2005; 127:8940. [PubMed: 15969557] (b) Kaye SS, Long JR. J. Am. Chem. Soc. 2008; 130:806. [PubMed: 18154339] (c) Tanabe KK, Cohen SM. Angew. Chem. Int. Ed. 2009; 48:7424.(d) Farrusseng D, Aguado S, Pinel C. Angew. Chem. Int. Ed. 2009; 48:7502.(e) Ma LQ, Folkowski JM, Abney C, Lin WB. Nat. Chem. 2010; 2:838. [PubMed: 20861899] (f) Oisaki K, Li Q, Furukawa H, Czaja AU, Yaghi OM. J. Am. Chem. Soc. 2010; 132:9262. [PubMed: 20557041]
10. (a) Taylor-Pashow KML, Della Rocca J, Xie ZG, Tran S, Lin WB. J. Am. Chem. Soc. 2009; 131:14261. [PubMed: 19807179] (b) Mckinlay AC, Xiao B, Wragg DS, Wheatley PS, Megson IL, Morris RE. J. Am. Chem. Soc. 2008; 130:10440. [PubMed: 18627150]
11. Zhao D, Tan S, Yuan D, Lu W, Rezenom YH, Jiang H, Wang LQ, Zhou HC. Adv. Mater. 2011; 23:90. [PubMed: 20972982]
12. (a) Wang M, Zheng Y-R, Ghosh K, Stang PJ. J. Am. Chem. Soc. 2010; 132:6282. [PubMed: 20405914] (b) Zhao Z, Zheng Y-R, Wang M, Pollock JB, Stang PJ. Inorg. Chem. 2010; 49:8653. [PubMed: 20809652] (c) Zheng Y-R, Zhao Z, Wang M, Ghosh K, Pollock JB, Stang PJ. J. Am. Chem. Soc. 2010; 132:11873.
13. Wang M, Zheng Y-R, Cook TR, Stang PJ. 2011 submitted.
14. (a) Ghosh K, Hu JM, White HS, Stang PJ. J. Am. Chem. Soc. 2009; 131:6695. [PubMed: 19397325] (b) Ghosh K, Hu JM, Yang HB, Northrop BH, White HS, Stang PJ. J. Org. Chem. 2009; 74:4828. [PubMed: 19485351] (c) Yang HB, Ghosh K, Zhao Y, Northrop BH, Lyndon MM, Muddiman DC, White HS, Stang PJ. J. Am. Chem. Soc. 2008; 130:839. [PubMed: 18166061]
15. Flanagan JB, Margel S, Bard AJ, Anson FC. J. Am. Chem. Soc. 1978; 100:4248.
16. Bard, AJ.; Faulkner, LR. Electrochemical Methods: Fundamentals and Applications. 2nd ed.. New York: John Wiley & Sons; 2001.
17. Denault G, Mirkin M, Bard AJ. J. Electroanal. Chem. 1991; 308:27.

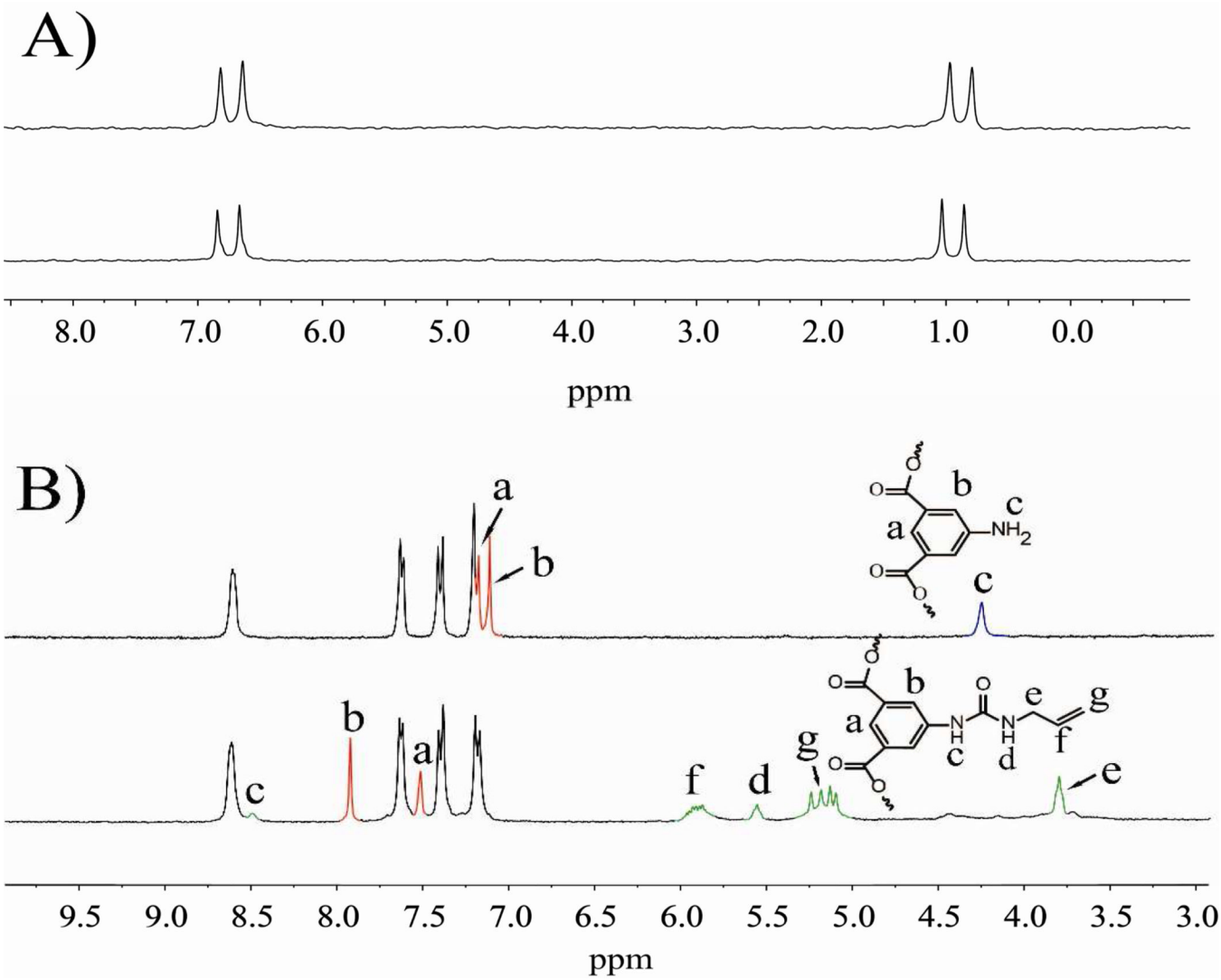

Figure 1.

A) $^{31}P\{^{1}H\}$ NMR spectra of hexagonal prisms **5** *(top)* and **7** (*bottom*) in acetonitrile-*d*3 (122.14 MHz, 298 K); *B*) Partial 1HNMR spectra of hexagonal prisms **5** *(top)* and **7** (*bottom*) in acetonitrile-*d*3 (300 MHz, 298 K).

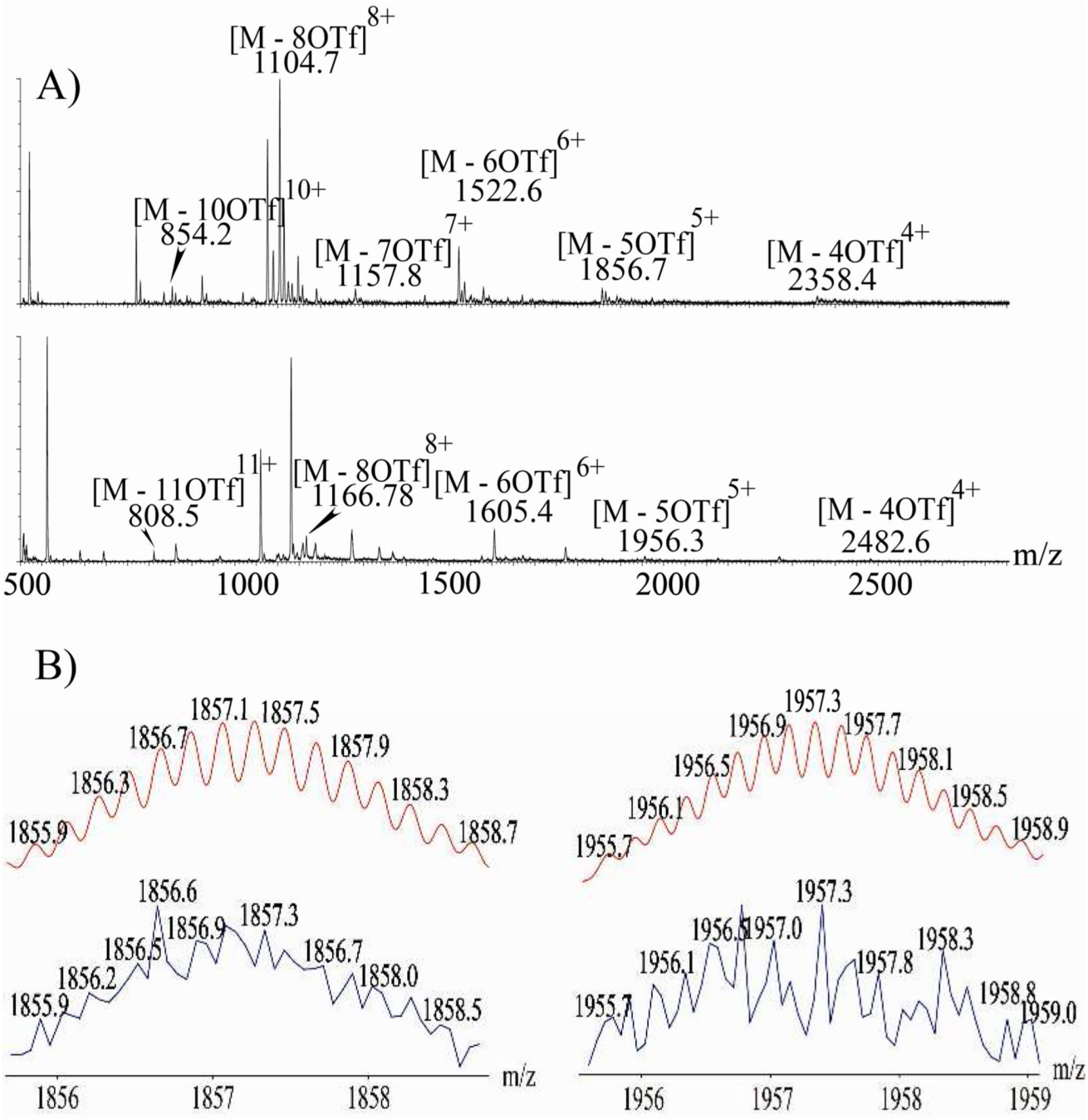

Figure 2.

ESI-MS spectra of hexagonal prism **5** and **7**: *A*) full MS spectra of **5** (*top*) and **7** (*bottom*); *B*) Calculated (*red*) and experimental (*blue*) mass spectra of [M- 5OTf]$^{5+}$ peak of **5** (*left*) and **7** (*right*).

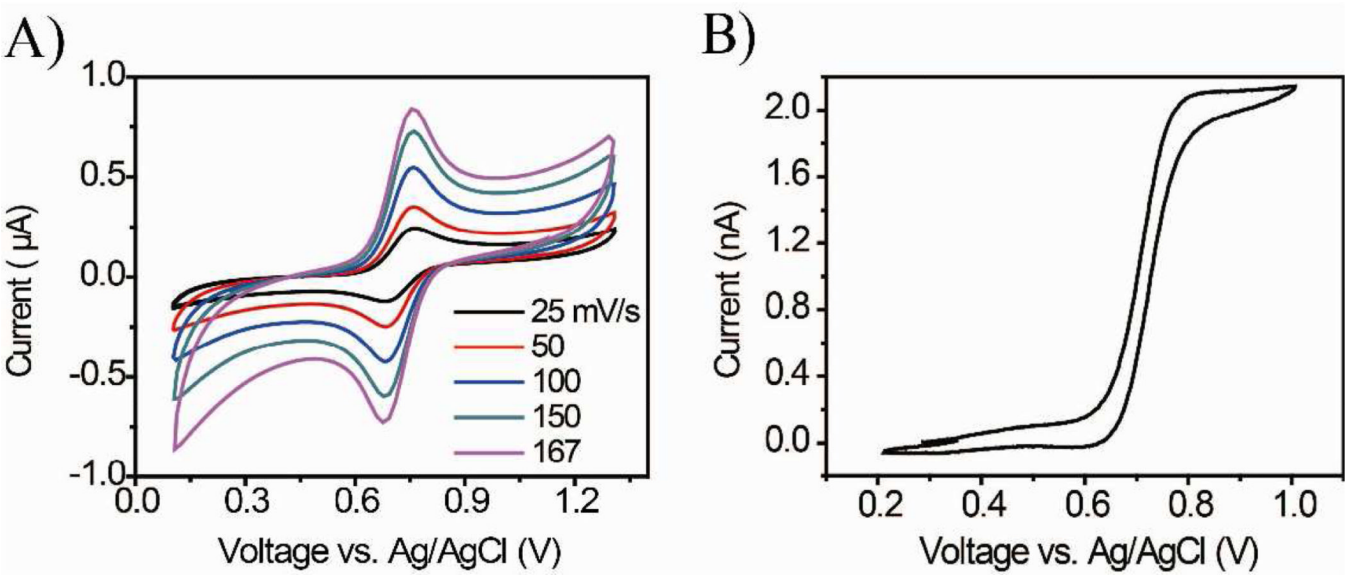

Figure 3.

(*A*) Cyclic voltametry of compound **10** at different scan rates (25–167 mV/s) at a ~0.5 mm^2 Pt electrode; (*B*) Steady-state current response of compound **10** at 30 mV/s at a ~ 25 μm diameter Pt disk electrode. Solution: 0.2 mM **10** in acetonitrile containing 0.1 M *n*-BuN_4PF_6.

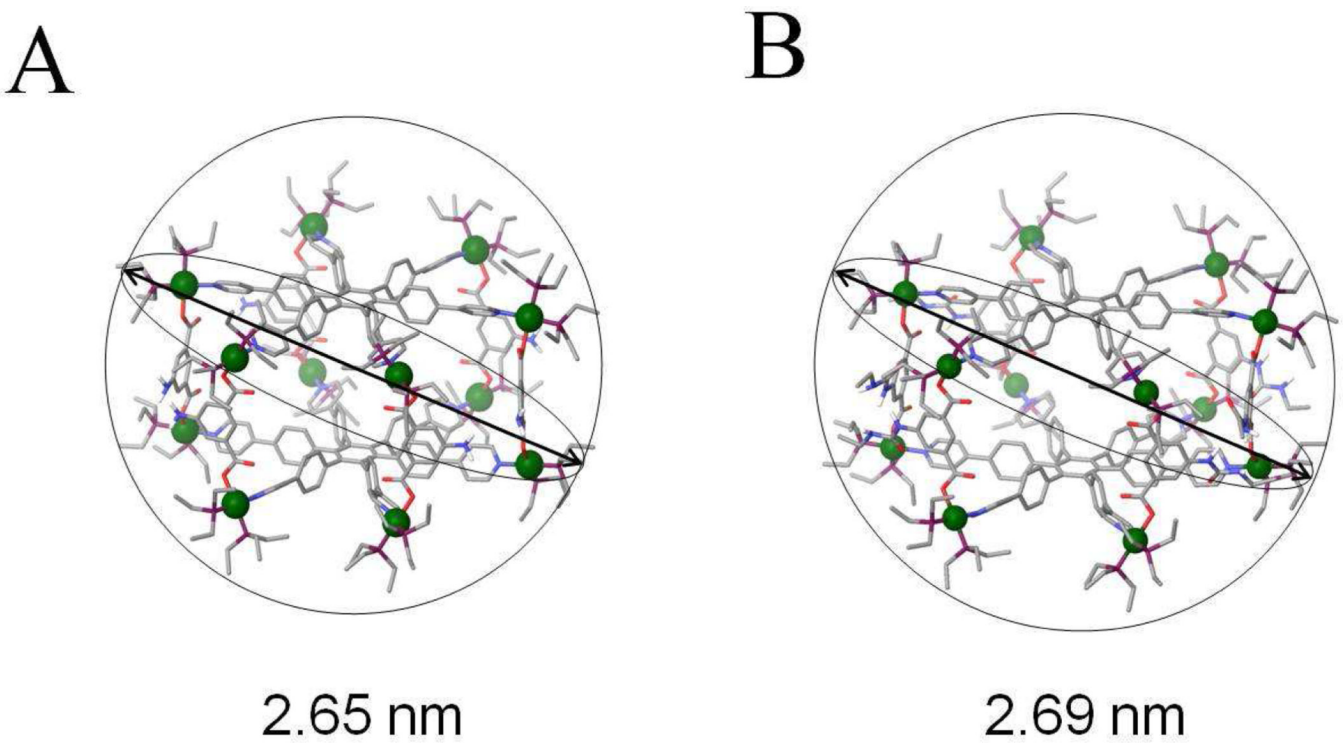

Figure 4.
Molecular modeling of hexagonal prisms **5** (*A*) and **7** (*B*).

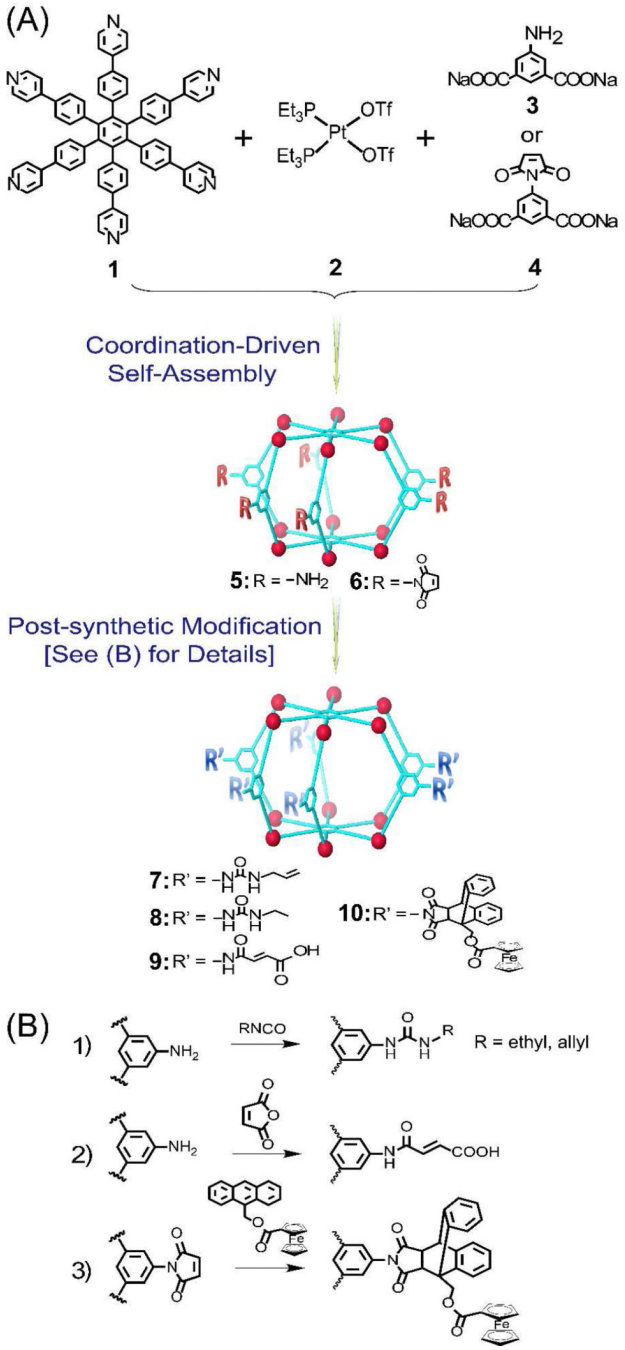

Scheme 1.

Illustration (A) and Chemical Principles (B) for the Post-synthetic Covalent Modifications of Discrete Multicomponent Metallosupramolecular Hexagonal Prisms